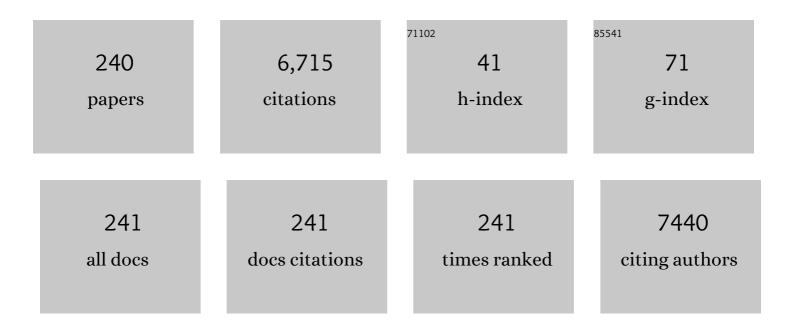
List of Publications by Year in descending order

Source: https://exaly.com/author-pdf/6550596/publications.pdf Version: 2024-02-01



YUNEEL CHEN

#	Article	IF	CITATIONS
1	Controllable preparation of dual-phase VC-C through in-situ electroconversion for lithium storage. Ceramics International, 2022, 48, 1024-1031.	4.8	3
2	Developing machine learning potential for classical molecular dynamics simulation with superior phonon properties. Computational Materials Science, 2022, 202, 111012.	3.0	3
3	Nanoscale friction behavior of monolayer MoxW1â^'xS2 alloy. Tribology International, 2022, 166, 107363.	5.9	2
4	Anisotropic phonon transport in van der Waals nanostructures. Physics Letters, Section A: General, Atomic and Solid State Physics, 2022, 427, 127920.	2.1	0
5	MoS ₂ /MXene Aerogel with Conformal Heterogeneous Interfaces Tailored by Atomic Layer Deposition for Tunable Microwave Absorption. Advanced Science, 2022, 9, e2101988.	11.2	76
6	Directional passive transport of nanodroplets on general axisymmetric surfaces. Physical Chemistry Chemical Physics, 2022, 24, 9727-9734.	2.8	4
7	Atomic Layer Deposition-Made MoS ₂ –ReS ₂ Nanotubes with Cylindrical Wall Heterojunctions for Ultrasensitive MiRNA-155 Detection. ACS Applied Materials & Interfaces, 2022, 14, 10081-10091.	8.0	7
8	Fabrication of solid-state nanopores. Nanotechnology, 2022, 33, 272003.	2.6	4
9	Van der Waals Magnetic Heterojunctions with Giant Zeroâ€Bias Tunneling Magnetoresistance and Photoâ€Assisted Magnetic Memory. Advanced Functional Materials, 2022, 32, .	14.9	4
10	Navigated Delivery of Peptide to the Nanopore Using In-Plane Heterostructures of MoS ₂ and SnS ₂ for Protein Sequencing. Journal of Physical Chemistry Letters, 2022, 13, 3863-3872.	4.6	11
11	Investigation of energy accommodation coefficient at gas-solid interface of a hypersonic flying vehicle. Aerospace Science and Technology, 2022, 126, 107585.	4.8	4
12	Encoding Manipulation of DNAâ€Nanoparticle Assembled Nanorobot Using Independently Charged Array Nanopores. Small Methods, 2022, 6, .	8.6	11
13	Facile preparation of metallic vanadium from consumable V2CO solid solution by molten salt electrolysis. Separation and Purification Technology, 2022, 295, 121361.	7.9	4
14	Monte Carlo Simulation of Naroline Thermal Conductivity Using a Conditional Variational Autoencoder. , 2022, , .		0
15	Direct ink writing of programmable functional siliconeâ€based composites for 4D printing applications. , 2022, 1, 507-516.		25
16	Heavy metal pollution and health risk assessment of agricultural land in the Southern Margin of Tarim Basin in Xinjiang, China. International Journal of Environmental Health Research, 2021, 31, 835-847.	2.7	12
17	Water quality and health risk assessment of shallow groundwater in the southern margin of the Tarim Basin in Xinjiang, P. R. China. Human and Ecological Risk Assessment (HERA), 2021, 27, 483-503.	3.4	11
18	Deubiquitinase USP35 restrains STING-mediated interferon signaling in ovarian cancer. Cell Death and Differentiation, 2021, 28, 139-155.	11.2	42

#	Article	IF	CITATIONS
19	Phonon transport in graphene based materials. Physical Chemistry Chemical Physics, 2021, 23, 26030-26060.	2.8	20
20	Electric control of ionic transport in sub-nm nanopores. RSC Advances, 2021, 11, 13806-13813.	3.6	2
21	Design and Manufacture of 3D-Printed Batteries. Joule, 2021, 5, 89-114.	24.0	137
22	A general strategy for designing two-dimensional high-efficiency layered thermoelectric materials. Energy and Environmental Science, 2021, 14, 4059-4066.	30.8	24
23	Green and sustainable molten salt electrochemistry for the conversion of secondary carbon pollutants to advanced carbon materials. Journal of Materials Chemistry A, 2021, 9, 14119-14146.	10.3	32
24	Concentration Polarization of High Concentration Solution in Sub-nm Nanopore. E3S Web of Conferences, 2021, 245, 03001.	0.5	0
25	Observation of superdiffusive phonon transport in aligned atomic chains. Nature Nanotechnology, 2021, 16, 764-768.	31.5	43
26	Size-Dependent Particle Separating in Curved Microfluidic Chip. , 2021, , .		0
27	Non-monotonic boundary resistivity for electron transport in metal nanowires. Applied Physics Letters, 2021, 118, 153105.	3.3	2
28	Resonance in Atomic-Scale Sliding Friction. Nano Letters, 2021, 21, 4615-4621.	9.1	20
29	The Thinnest Light Disk: Rewritable Data Storage and Encryption on WS ₂ Monolayers. Advanced Functional Materials, 2021, 31, 2103140.	14.9	7
30	DNA Damage Repair Status Predicts Opposite Clinical Prognosis Immunotherapy and Non-Immunotherapy in Hepatocellular Carcinoma. Frontiers in Immunology, 2021, 12, 676922.	4.8	15
31	Detection and Separation of Single-Stranded DNA Fragments Using Solid-State Nanopores. Journal of Physical Chemistry Letters, 2021, 12, 6469-6477.	4.6	10
32	Analysis of Interleukin-1 Signaling Alterations of Colon Adenocarcinoma Identified Implications for Immunotherapy. Frontiers in Immunology, 2021, 12, 665002.	4.8	1
33	Manipulating valley-polarized photoluminescence of MoS2 monolayer at off resonance wavelength with a double-resonance strategy. Applied Physics Letters, 2021, 119, 031106.	3.3	7
34	Surface Charge Density Inside a Silicon Nitride Nanopore. Langmuir, 2021, 37, 10521-10528.	3.5	15
35	The Thinnest Light Disk: Rewritable Data Storage and Encryption on WS ₂ Monolayers (Adv.) Tj ETC	Qq110.78 14.9	4314 rgBT /0
36	Dual-phase MoC-Mo2C nanosheets prepared by molten salt electrochemical conversion of CO2 as	16.0	48

excellent electrocatalysts for the hydrogen evolution reaction. Nano Energy, 2021, 90, 106533.

16.0 48

YUNFEI CHEN

#	Article	IF	CITATIONS
37	Modulating thermal conductance across the metal/graphene/SiO ₂ interface with ion irradiation. Physical Chemistry Chemical Physics, 2021, 23, 22760-22767.	2.8	4
38	Synergic Effects of the Nanopore Size and Surface Charge on the Ion Selectivity of Graphene Membranes. Journal of Physical Chemistry C, 2021, 125, 507-514.	3.1	11
39	Computational design of a hydrogenated porous graphene membrane for anion selective transport. , 2021, , .		1
40	Experimental measurements on the thermal conductivity of strained monolayer graphene. Carbon, 2020, 157, 185-190.	10.3	51
41	Theory of aerodynamic heating from molecular collision analysis. Physics Letters, Section A: General, Atomic and Solid State Physics, 2020, 384, 126098.	2.1	2
42	Phonon energy dissipation in friction between graphene/graphene interface. Journal of Applied Physics, 2020, 127, .	2.5	24
43	Shape characterization and discrimination of single nanoparticles using solid-state nanopores. Analyst, The, 2020, 145, 1657-1666.	3.5	12
44	Electrochemical graphitization conversion of CO2 through soluble NaVO3 homogeneous catalyst in carbonate molten salt. Electrochimica Acta, 2020, 331, 135461.	5.2	26
45	The effects of contact atom distribution at the interface on the phonon transport. Physical Chemistry Chemical Physics, 2020, 22, 27690-27697.	2.8	3
46	Bidirectional Tuning of Thermal Conductivity in Ferroelectric Materials Using E-Controlled Hysteresis Characteristic Property. Journal of Physical Chemistry C, 2020, 124, 26144-26152.	3.1	23
47	Investigation of Ergonomics in Photocuring 3D Printing Post-Processing Using Jack. , 2020, , .		3
48	Design of LED Collimating lens for uniform illumination with freeform surface. , 2020, , .		1
49	Experimental measurement of thermal conductivity along different crystallographic planes in graphite. Journal of Applied Physics, 2020, 128, .	2.5	6
50	Water-ion permselectivity of narrow-diameter carbon nanotubes. Science Advances, 2020, 6, .	10.3	58
51	Inside Back Cover: Detergentâ€Assisted Braking of Peptide Translocation through a Singleâ€Layer Molybdenum Disulfide Nanopore (Small Methods 11/2020). Small Methods, 2020, 4, 2070043.	8.6	0
52	A Nanoparticle-DNA Assembled Nanorobot Powered by Charge-Tunable Quad-Nanopore System. ACS Nano, 2020, 14, 15349-15360.	14.6	30
53	Ion Concentration Effect on Nanoscale Electrospray Modes. Small, 2020, 16, e2000397.	10.0	11
54	Significant enhancement of thermal boundary conductance in graphite/Al interface by ion intercalation. International Journal of Heat and Mass Transfer, 2020, 157, 119946.	4.8	12

#	Article	IF	CITATIONS
55	Experimental Study on Strengthening Carbothermic Reduction of Vanadium-Titanium-Magnetite by Adding CaF2. Minerals (Basel, Switzerland), 2020, 10, 219.	2.0	11
56	The enhancement of heat conduction across the metal/graphite interface treated with a focused ion beam. Nanoscale, 2020, 12, 14838-14846.	5.6	12
57	Thermal boundary conductance between high thermal conductivity boron arsenide and silicon. Journal of Applied Physics, 2020, 127, 055105.	2.5	6
58	Detergentâ€Assisted Braking of Peptide Translocation through a Singleâ€Layer Molybdenum Disulfide Nanopore. Small Methods, 2020, 4, 1900822.	8.6	16
59	Charge Inversion and Calcium Gating in Mixtures of Ions in Nanopores. Journal of the American Chemical Society, 2020, 142, 2925-2934.	13.7	73
60	Thermal protection of a hypersonic vehicle by modulating stagnation-point heat flux. Aerospace Science and Technology, 2020, 98, 105673.	4.8	14
61	Strong Differential Monovalent Anion Selectivity in Narrow Diameter Carbon Nanotube Porins. ACS Nano, 2020, 14, 6269-6275.	14.6	35
62	High ZT 2D Thermoelectrics by Design: Strong Interlayer Vibration and Complete Bandâ€Extrema Alignment. Advanced Functional Materials, 2020, 30, 2001200.	14.9	32
63	The ignored effects of vibrational entropy and electrocaloric effect in PbTiO3 and PbZr0.5Ti0.5O3 as studied through first-principles calculation. Acta Materialia, 2020, 191, 221-229.	7.9	18
64	Electroosmotic Facilitated Protein Capture and Transport through Solid‧tate Nanopores with Diameter Larger than Length. Small Methods, 2020, 4, 1900893.	8.6	26
65	Diminishing Cohesion of Chitosan Films in Acidic Solution by Multivalent Metal Cations. Langmuir, 2020, 36, 4964-4974.	3.5	5
66	Fluid release pressure for micro-/nanoscale rectangular channels. Journal of Applied Physics, 2020, 127, .	2.5	2
67	Inter- and intramolecular adhesion mechanisms of mussel foot proteins. Science China Technological Sciences, 2020, 63, 1675-1698.	4.0	14
68	Exosomal miR-29b from cancer-associated fibroblasts inhibits the migration and invasion of hepatocellular carcinoma cells. Translational Cancer Research, 2020, 9, 2576-2587.	1.0	12
69	Molecular dynamics study on the effect of lipid membrane mechanical properties on the interaction between Î ² -amyloid and lipid membrane. , 2020, , .		0
70	Effects of Commensurability on the Friction and Energy Dissipation in Graphene/Graphene Interface. , 2020, , .		2
71	Electrical and thermal conductivities of polycrystalline platinum nanowires. Nanotechnology, 2019, 30, 455706.	2.6	5
72	Analysis of reciprocating Oâ€ring seal in the pressureâ€balanced oilâ€filled wetâ€mate electrical connectors for underwater applications. Lubrication Science, 2019, 31, 335-345.	2.1	7

#	Article	IF	CITATIONS
73	Factors influencing the distribution of arsenic, fluorine and iodine in shallow groundwater in the oasis zone in the southern margin of the Tarim Basin in Xinjiang, P. R. China. E3S Web of Conferences, 2019, 98, 09006.	0.5	0
74	New Insight on the Interface between Polythiophene and Semiconductors via Molecular Dynamics Simulations. ACS Applied Materials & Interfaces, 2019, 11, 30470-30476.	8.0	9
75	A Comparative Study of Water Quality and Human Health Risk Assessment in Longevity Area and Adjacent Non-Longevity Area. International Journal of Environmental Research and Public Health, 2019, 16, 3737.	2.6	6
76	Passive microscopic fluidic diodes using asymmetric channels. AIP Advances, 2019, 9, 085117.	1.3	4
77	Thermal Bubble Nucleation in Graphene Nanochannels. Journal of Physical Chemistry C, 2019, 123, 3482-3490.	3.1	11
78	Glycerol-Assisted Construction of Long-Life Three-Dimensional Surface-Enhanced Raman Scattering Hot Spot Matrix. Langmuir, 2019, 35, 15795-15804.	3.5	8
79	Effects of Surface Trapping and Contact Ion Pairing on Ion Transport in Nanopores. Journal of Physical Chemistry C, 2019, 123, 15314-15322.	3.1	17
80	Sulfurâ€Mastery: Precise Synthesis of 2D Transition Metal Dichalcogenides. Advanced Functional Materials, 2019, 29, 1809261.	14.9	36
81	Ubiquitination of cGAS by TRAF6 regulates anti-DNA viral innate immune responses. Biochemical and Biophysical Research Communications, 2019, 514, 659-664.	2.1	24
82	Discrimination of Protein Amino Acid or Its Protonated State at Singleâ€Residue Resolution by Graphene Nanopores. Small, 2019, 15, e1900036.	10.0	33
83	High Curie temperature and intrinsic ferromagnetic half-metallicity in two-dimensional Cr ₃ X ₄ (X = S, Se, Te) nanosheets. Nanoscale Horizons, 2019, 4, 859-866.	8.0	84
84	Direct detection of DNA using 3D surface enhanced Raman scattering hotspot matrix. Electrophoresis, 2019, 40, 2104-2111.	2.4	7
85	Electric-Field-Controlled Thermal Switch in Ferroelectric Materials Using First-Principles Calculations and Domain-Wall Engineering. Physical Review Applied, 2019, 11, .	3.8	42
86	Fluid release pressure for nanochannels: the Young–Laplace equation using the effective contact angle. Nanoscale, 2019, 11, 8408-8415.	5.6	35
87	Kink effects on thermal transport in silicon nanowires. International Journal of Heat and Mass Transfer, 2019, 137, 573-578.	4.8	12
88	Nanotribological Properties of ALD-Made Ultrathin MoS ₂ Influenced by Film Thickness and Scanning Velocity. Langmuir, 2019, 35, 3651-3657.	3.5	16
89	Drastically Reduced Ion Mobility in a Nanopore Due to Enhanced Pairing and Collisions between Dehydrated Ions. Journal of the American Chemical Society, 2019, 141, 4264-4272.	13.7	46
90	Discrimination of singleâ€stranded DNA homopolymers by sieving out Gâ€quadruplex using tiny solidâ€state nanopores. Electrophoresis, 2019, 40, 2117-2124.	2.4	10

#	Article	lF	CITATIONS
91	An Nd3+-Sensitized Upconversion Fluorescent Sensor for Epirubicin Detection. Nanomaterials, 2019, 9, 1700.	4.1	10
92	Computational modeling of ionic currents through difform graphene nanopores with consistent cross-sectional areas. Physical Chemistry Chemical Physics, 2019, 21, 26166-26174.	2.8	5
93	Size Characterization of Single Nanoparticles Using Solid-state Nanopores. , 2019, , .		0
94	AFM Study of Temperature and pH Effects on BSA Structure and Adhesion. , 2019, , .		0
95	Fabrication of Nanopores Using Controlled Dielectric Breakdown. , 2019, , .		1
96	Reduction of electrical conductivity in Ag nanowires induced by low-energy electron beam irradiation. Journal of Physics and Chemistry of Solids, 2019, 124, 89-93.	4.0	5
97	Mechanisms of pressure-induced water infiltration process through graphene nanopores. Molecular Simulation, 2019, 45, 518-524.	2.0	3
98	Distinct Signatures of Electron–Phonon Coupling Observed in the Lattice Thermal Conductivity of NbSe ₃ Nanowires. Nano Letters, 2019, 19, 415-421.	9.1	37
99	Tuning the interfacial thermal conductance via the anisotropic elastic properties of graphite. Carbon, 2019, 144, 109-115.	10.3	20
100	Reliability and Simulation of composite BGA solder joint connecting LTCC substrates. , 2019, , .		1
101	Fabrication of sub-nanometer pores on graphene membrane for ion selective transport. Nanoscale, 2018, 10, 5350-5357.	5.6	50
102	Thermal Transport in Quasi-1D van der Waals Crystal Ta ₂ Pd ₃ Se ₈ Nanowires: Size and Length Dependence. ACS Nano, 2018, 12, 2634-2642.	14.6	61
103	Study of the reduction mechanism of ironsands with addition of blast furnace bag dust. Metallurgical Research and Technology, 2018, 115, 214.	0.7	4
104	Transient and steady state heat transport in layered materials from molecular dynamics simulation. International Journal of Heat and Mass Transfer, 2018, 121, 72-78.	4.8	8
105	Tunable Anisotropic Thermal Conductivity and Elastic Properties in Intercalated Graphite via Lithium Ions. Journal of Physical Chemistry C, 2018, 122, 1447-1455.	3.1	22
106	Optimal design of graphene nanopores for seawater desalination. Journal of Chemical Physics, 2018, 148, 014703.	3.0	30
107	Effect of Electrical Contact Resistance on Measurement of Thermal Conductivity and Wiedemann-Franz Law for Individual Metallic Nanowires. Scientific Reports, 2018, 8, 4862.	3.3	29
108	Intermittent Pringle Versus Continuous Half-Pringle Maneuver for Laparoscopic Liver Resections of Tumors in Segment 7. Indian Journal of Surgery, 2018, 80, 146-153.	0.3	4

#	Article	IF	CITATIONS
109	Selective ion-permeation through strained and charged graphene membranes. Nanotechnology, 2018, 29, 035402.	2.6	14
110	The frictional energy dissipation and interfacial heat conduction in the sliding interface. AIP Advances, 2018, 8, .	1.3	9
111	Identification of Spherical and Nonspherical Proteins by a Solid-State Nanopore. Analytical Chemistry, 2018, 90, 13826-13831.	6.5	52
112	Thermal transport in electrospun vinyl polymer nanofibers: effects of molecular weight and side groups. Soft Matter, 2018, 14, 9534-9541.	2.7	27
113	Controllable and reversible DNA translocation through a single-layer molybdenum disulfide nanopore. Nanoscale, 2018, 10, 19450-19458.	5.6	37
114	Bi ₂ OS ₂ : a direct-gap two-dimensional semiconductor with high carrier mobility and surface electron states. Materials Horizons, 2018, 5, 1058-1064.	12.2	45
115	Large Thermal Conductivity Switch Ratio in Barium Titanate Under Electric Field through Firstâ€Principles Calculation. Advanced Theory and Simulations, 2018, 1, 1800098.	2.8	23
116	Identification of Single Nucleotides by a Tiny Charged Solid-State Nanopore. Journal of Physical Chemistry B, 2018, 122, 7929-7935.	2.6	20
117	MoS2 solid-lubricating film fabricated by atomic layer deposition on Si substrate. AIP Advances, 2018, 8, .	1.3	16
118	Evaluating the cognitive process of color affordance and attractiveness based on the ERP. International Journal on Interactive Design and Manufacturing, 2017, 11, 471-479.	2.2	9
119	Hydrophobic copper nanowires for enhancing condensation heat transfer. Nano Energy, 2017, 33, 177-183.	16.0	181
120	Preparation and characterization of molybdenum disulfide films obtained by one-step atomic layer deposition method. Thin Solid Films, 2017, 624, 101-105.	1.8	28
121	Axial tensile strain effects on the contact thermal conductance between cross contacted single-walled carbon nanotubes. Journal of Applied Physics, 2017, 121, .	2.5	2
122	Defect Facilitated Phonon Transport through Kinks in Boron Carbide Nanowires. Nano Letters, 2017, 17, 3550-3555.	9.1	23
123	Salt Gradient Improving Signal-to-Noise Ratio in Solid-State Nanopore. ACS Sensors, 2017, 2, 506-512.	7.8	27
124	Mean free path dependent phonon contributions to interfacial thermal conductance. Physics Letters, Section A: General, Atomic and Solid State Physics, 2017, 381, 1899-1904.	2.1	23
125	Layer-controlled precise fabrication of ultrathin MoS ₂ films by atomic layer deposition. Nanotechnology, 2017, 28, 195605.	2.6	39
126	lonic current modulation from DNA translocation through nanopores under high ionic strength and concentration gradients. Nanoscale, 2017, 9, 930-939.	5.6	32

#	Article	IF	CITATIONS
127	Photoluminescence characterization of the grain boundary thermal stability in chemical vapor deposition grown WS ₂ . Materials Research Express, 2017, 4, 106202.	1.6	8
128	A convenient method of manufacturing liquid-gated MoS ₂ field effect transistors. Materials Research Express, 2017, 4, 105028.	1.6	5
129	Phonon transport properties of bulk and monolayer GaN from first-principles calculations. Computational Materials Science, 2017, 138, 419-425.	3.0	39
130	Phonon filtering for reduced thermal conductance in unconventional superlattices. Applied Physics Express, 2017, 10, 085801.	2.4	3
131	Fabrication of liquid-gated molybdenum disulfide field-effect transistor. , 2017, , .		2
132	High-Performance Graphene-Based Electrostatic Field Sensor. IEEE Electron Device Letters, 2017, 38, 1136-1138.	3.9	12
133	Investigation on the interaction length and access resistance of a nanopore with an atomic force microscopy. Science China Technological Sciences, 2017, 60, 552-560.	4.0	12
134	Thermal transport properties of all-sp2 three-dimensional graphene: Anisotropy, size and pressure effects. Carbon, 2017, 113, 212-218.	10.3	31
135	Distribution of groundwater arsenic in Xinjiang, P.R. China. Applied Geochemistry, 2017, 77, 116-125.	3.0	35
136	Force measurements between mica surfaces in concentrated electrolyte solutions. , 2017, , .		0
137	Surface force apparatus studies on the surface interaction of [C<inf>n</inf>mim ⁺][BF<inf>4</inf> ^{â^'}] and [C<inf>n</inf>mim ⁺]][PF<inf>6</inf> ^{â^'}] ionic liquids., 2017		0
138	Experimental Research of Protein Translocation Using Solid-state Nanopore. Acta Chimica Sinica, 2017, 75, 1121.	1.4	5
139	Pressure Effects on the Thermal Properties of Graphite. , 2016, , .		0
140	Direction Dependence of Resistive-Pulse Amplitude in Conically Shaped Mesopores. Analytical Chemistry, 2016, 88, 4917-4925.	6.5	42
141	Ionic Behavior in Highly Concentrated Aqueous Solutions Nanoconfined between Discretely Charged Silicon Surfaces. Langmuir, 2016, 32, 4806-4814.	3.5	26
142	Thermal conductivity of individual silicon nanoribbons. Nanoscale, 2016, 8, 17895-17901.	5.6	54
143	Thermal transport across symmetric and asymmetric solid–solid interfaces. Applied Physics A: Materials Science and Processing, 2016, 122, 1.	2.3	7
144	Geometric tuning of thermal conductivity in three-dimensional anisotropic phononic crystals. Nanoscale, 2016, 8, 16612-16620.	5.6	22

#	Article	IF	CITATIONS
145	Carrier dynamics in femtosecond-laser-excited bismuth telluride. Physical Review B, 2016, 93, .	3.2	10
146	Intermittent Pringle maneuver versus continuous hemihepatic vascular inflow occlusion using extra-glissonian approach in laparoscopic liver resection. Surgical Endoscopy and Other Interventional Techniques, 2016, 30, 961-970.	2.4	25
147	Pressure effects on the thermal resistance of few-layer graphene. Physics Letters, Section A: General, Atomic and Solid State Physics, 2016, 380, 248-254.	2.1	16
148	Effects of interfacial roughness on phonon transport in bilayer silicon thin films. Physical Review B, 2015, 92, . Detection of short single strand DNA homopolymers with ultrathins multimath	3.2	14
149	xmlns:mml="http://www.w3.org/1998/Math/MathML"> <mml:mrow> <mml:mi mathvariant="normal">S <mml:msub> <mml:mi mathvariant="normal">i <mml:mn>3</mml:mn> </mml:mi </mml:msub> <mml:msub> <mml:mi mathvariant="normal">N <mml:mn> 4</mml:mn> </mml:mi </mml:msub> </mml:mi </mml:mrow> nanopores.	2.1	16
150	Physical Review E, 2015, 92, 022719. Phonon transport properties in pillared silicon film. Journal of Applied Physics, 2015, 118, .	2.5	38
151	Structure and properties of water film adsorbed on mica surfaces. Journal of Chemical Physics, 2015, 143, 104705.	3.0	32
152	Influence of coherent optical phonon on ultrafast energy relaxation. Applied Physics Letters, 2015, 107, 063107.	3.3	4
153	The contact area dependent interfacial thermal conductance. AIP Advances, 2015, 5, .	1.3	10
154	Cross-plane phonon transport properties of molybdenum disulphide. Journal Physics D: Applied Physics, 2015, 48, 465303.	2.8	5
155	Study of DNA adsorption on mica surfaces using a surface force apparatus. Scientific Reports, 2015, 5, 8442.	3.3	31
156	Experimental evidence of very long intrinsic phonon mean free path along the <i>c</i> -axis of graphite. Applied Physics Letters, 2015, 106, .	3.3	58
157	A microfluidic device for generation of chemical gradients. Microsystem Technologies, 2015, 21, 1797-1804.	2.0	7
158	Experimental and Theoretical Investigations on the Nanoscale Kinetic Friction in Ambient Environmental Conditions. Nano Letters, 2015, 15, 4704-4712.	9.1	13
159	Defect-Engineered Heat Transport in Graphene: A Route to High Efficient Thermal Rectification. Scientific Reports, 2015, 5, 11962.	3.3	96
160	Glass capillary nanopore for single molecule detection. Science China Technological Sciences, 2015, 58, 803-812.	4.0	23
161	Manipulation of interfacial thermal conductance via Rhodamine 6G. Science Bulletin, 2015, 60, 654-656.	9.0	1
162	Thermal conductivity of electrospun polyethylene nanofibers. Nanoscale, 2015, 7, 16899-16908.	5.6	103

#	Article	IF	CITATIONS
163	Capacitance Performance of Sub-2 nm Graphene Nanochannels in Aqueous Electrolyte. Journal of Physical Chemistry C, 2015, 119, 23813-23819.	3.1	25
164	Wafer-level site-controlled growth of silicon nanowires by Cu pattern dewetting. Nano Research, 2015, 8, 2646-2653.	10.4	4
165	Totally Laparoscopic Associating Liver Tourniquet and Portal Ligation for Staged Hepatectomy via Anterior Approach for Cirrhotic Hepatocellular Carcinoma. Journal of the American College of Surgeons, 2015, 221, e43-e48.	0.5	9
166	Thermal conductivity of zinc blende and wurtzite CdSe nanostructures. Nanoscale, 2015, 7, 16071-16078.	5.6	11
167	Temperature effect on translocation speed and capture rate of nanopore-based DNA detection. Science China Technological Sciences, 2015, 58, 519-525.	4.0	10
168	Counterions and water molecules in charged silicon nanochannels: the influence of surface charge discreteness. Molecular Simulation, 2015, 41, 1187-1192.	2.0	6
169	Wafer-lever Au Nanogap-Nanopore Fabricated by NEMS Technology. , 2015, , .		0
170	Retarding and manipulating of DNA molecules translocation through nanopores. Science Bulletin, 2014, 59, 4908-4917.	1.7	7
171	Molecular Dynamics Studies of Homogeneous and Heterogeneous Thermal Bubble Nucleation. Journal of Heat Transfer, 2014, 136, .	2.1	13
172	Integrated solid-state nanopore devices for third generation DNA sequencing. Science China Technological Sciences, 2014, 57, 1925-1935.	4.0	7
173	Phonon mean free path of graphite along the <i>c</i> -axis. Applied Physics Letters, 2014, 104, 081903.	3.3	67
174	DNA sequencing technology based on nanopore sensors by theoretical calculations and simulations. Science Bulletin, 2014, 59, 4929-4941.	1.7	12
175	Imaging the condensation and evaporation of molecularly thin ethanol films with surface forces apparatus. Review of Scientific Instruments, 2014, 85, 013702.	1.3	2
176	Theoretical and experimental studies on ionic currents in nanoporeâ€based biosensors. IET Nanobiotechnology, 2014, 8, 247-256.	3.8	2
177	Intramolecular C–H Bond Activation in Bridged Dicyclopentadienyl Dimethyl Dinuclear Complexes. Organometallics, 2014, 33, 240-248.	2.3	7
178	Mode dependent lattice thermal conductivity of single layer graphene. Journal of Applied Physics, 2014, 116, .	2.5	61
179	Experimental Observation of the Ion–Ion Correlation Effects on Charge Inversion and Strong Adhesion between Mica Surfaces in Aqueous Electrolyte Solutions. Langmuir, 2014, 30, 10845-10854.	3.5	57
180	Phonon Transport through Point Contacts between Graphitic Nanomaterials. Physical Review Letters, 2014, 112, .	7.8	60

#	Article	IF	CITATIONS
181	Ion specificity in NaCl solution confined in silicon nanochannels. Science China Technological Sciences, 2014, 57, 230-238.	4.0	10
182	Immunoglobulin Molecules Detection with Nanopore Sensors Fabricated from Glass Tubes. Journal of Nanoscience and Nanotechnology, 2014, 14, 4043-4049.	0.9	4
183	Boronate Complex Formation with Dopa Containing Mussel Adhesive Protein Retards pH-Induced Oxidation and Enables Adhesion to Mica. PLoS ONE, 2014, 9, e108869.	2.5	51
184	Molecular dynamics study of DNA translocation through graphene nanopores. Physical Review E, 2013, 87, 062707.	2.1	38
185	Heat transfer and pressure drop of nanofluids containing carbon nanotubes in laminar flows. Experimental Thermal and Fluid Science, 2013, 44, 716-721.	2.7	166
186	Nanopore detection of DNA molecules in magnesium chloride solutions. Nanoscale Research Letters, 2013, 8, 245.	5.7	27
187	Nanotubes Complexed with DNA and Proteins for Resistive-Pulse Sensing. ACS Nano, 2013, 7, 8857-8869.	14.6	30
188	Effect of nanopore size on poly(dT)30 translocation through silicon nitride membrane. Science China Technological Sciences, 2013, 56, 2398-2402.	4.0	21
189	Heat conduction across metal and nonmetal interface containing imbedded graphene layers. Carbon, 2013, 64, 61-66.	10.3	36
190	Negative correlation between in-plane bonding strength and cross-plane thermal conductivity in a model layered material. Applied Physics Letters, 2013, 102, .	3.3	50
191	Adaptive hydrophobic and hydrophilic interactions of mussel foot proteins with organic thin films. Proceedings of the National Academy of Sciences of the United States of America, 2013, 110, 15680-15685.	7.1	242
192	Simulations of the anisotropy of friction force between a silicon tip and a substrate at nanoscale. Proceedings of the Institution of Mechanical Engineers, Part N: Journal of Nanoengineering and Nanosystems, 2013, 227, 130-134.	0.1	2
193	Ionic current investigation in silicon nanochannels with molecular dynamics simulations. , 2013, , .		Ο
194	Water and ion distributions in a silicon nanochannel: a molecular dynamics study. Proceedings of the Institution of Mechanical Engineers, Part N: Journal of Nanoengineering and Nanosystems, 2012, 226, 31-34.	0.1	2
195	Wave packet simulations of phonon boundary scattering at graphene edges. Journal of Applied Physics, 2012, 112, 024328.	2.5	29
196	The Effects of Van Der Waals Bonding Strength on the In-Plane Lattice Thermal Conductivities of Multilayer Thin Films. , 2012, , .		0
197	The Phonon Thermal Conductivity of Single-Layer Graphene From Complete Phonon Dispersion Relations. Journal of Heat Transfer, 2012, 134, .	2.1	7
198	Enhancing Flow Boiling Heat Transfer in Microchannels for Thermal Management with Monolithically-Integrated Silicon Nanowires. Nano Letters, 2012, 12, 3385-3390.	9.1	181

#	Article	IF	CITATIONS
199	Reactions of Doubly SiMe2-Bridged Bis(cyclopentadienyl) Complexes of Molybdenum and Iron Carbonyls: Competitive Ring-to-Metal Migrations of Hydrogen and SiMe2. Organometallics, 2012, 31, 4046-4054.	2.3	8
200	Reactions of SnMe ₂ -Bridged Bis(cyclopentadienes) with Iron Pentacarbonyl: Migration of the SnMe ₂ Group. Organometallics, 2012, 31, 3035-3042.	2.3	5
201	The thermal conductivity of SiGe heterostructure nanowires with different cores and shells. Physics Letters, Section A: General, Atomic and Solid State Physics, 2012, 376, 2668-2671.	2.1	13
202	Measurement of thermal boundary conductance between metal and dielectric materials using femtosecond laser transient thermoreflectance technique. Science China Technological Sciences, 2012, 55, 1044-1049.	4.0	8
203	Enhanced and switchable nanoscale thermal conduction due to van der Waals interfaces. Nature Nanotechnology, 2012, 7, 91-95.	31.5	120
204	Effect of thermal coarsening on the thermal conductivity of nanoporous gold. Journal of Materials Science, 2012, 47, 5013-5018.	3.7	26
205	Interfacial thermal resistance in multilayer graphene structures. Physics Letters, Section A: General, Atomic and Solid State Physics, 2011, 375, 1195-1199.	2.1	106
206	Measurement of the Intrinsic Thermal Conductivity of a Multiwalled Carbon Nanotube and Its Contact Thermal Resistance with the Substrate. Small, 2011, 7, 2334-2340.	10.0	75
207	In-plane lattice thermal conductivities of multilayer graphene films. Carbon, 2011, 49, 2653-2658.	10.3	156
208	The effect of surface roughness on lattice thermal conductivity of silicon nanowires. Physica B: Condensed Matter, 2011, 406, 2515-2520.	2.7	24
209	A novel method of fabricating a nanopore based on a glass tube for single-molecule detection. Nanotechnology, 2011, 22, 175304.	2.6	18
210	Monte Carlo simulation of phonon transport in variable cross-section nanowires. Science China Technological Sciences, 2010, 53, 429-434.	4.0	10
211	Anisotropic mechanical properties of graphene sheets from molecular dynamics. Physica B: Condensed Matter, 2010, 405, 1301-1306.	2.7	248
212	Contact thermal resistance between individual multiwall carbon nanotubes. Applied Physics Letters, 2010, 96, .	3.3	134
213	A Modified Thermal Boundary Resistance Model for FCC Structures. , 2009, , .		0
214	Temperature dependence of frictional force in carbon nanotube oscillators. Nanotechnology, 2009, 20, 035704.	2.6	20
215	Atomistic simulations of mechanical properties of graphene nanoribbons. Physics Letters, Section A: General, Atomic and Solid State Physics, 2009, 373, 3359-3362.	2.1	144
216	Interface slip and the buildup of hydrodynamic pressure in nanoscale bearings. Physica B: Condensed Matter, 2009, 404, 231-234.	2.7	2

YUNFEI CHEN

#	Article	IF	CITATIONS
217	Water structures near charged (100) and (111) silicon surfaces. Applied Physics Letters, 2009, 94, .	3.3	18
218	Role of Tilted Adhesion Fibrils (Setae) in the Adhesion and Locomotion of Gecko-like Systems. Journal of Physical Chemistry B, 2009, 113, 3615-3621.	2.6	70
219	Ionic current through a nanopore three nanometers in diameter. Physical Review E, 2009, 80, 021918.	2.1	13
220	Frictional Adhesion of Patterned Surfaces and Implications for Gecko and Biomimetic Systems. Langmuir, 2009, 25, 7486-7495.	3.5	75
221	Ionic Current Through a 3 NM in Diameter Nanopore. , 2009, , .		0
222	Molecular dynamics simulation of ion transport in a nanochannel. Science in China Series D: Earth Sciences, 2008, 51, 921-931.	0.9	5
223	Electroosmotic Flow in Nanotubes with High Surface Charge Densities. Nano Letters, 2008, 8, 42-48.	9.1	67
224	Optimization of Superlattice Thermoelectric Materials and Microcoolers. Journal of Microelectromechanical Systems, 2007, 16, 1113-1119.	2.5	17
225	Thermal conductivities of single-walled carbon nanotubes calculated from the complete phonon dispersion relations. Physical Review B, 2007, 76, .	3.2	40
226	GPU accelerated molecular dynamics simulation of thermal conductivities. Journal of Computational Physics, 2007, 221, 799-804.	3.8	104
227	Molecular dynamics simulation of the test of single-walled carbon nanotubes under tensile loading. Science in China Series D: Earth Sciences, 2007, 50, 7-17.	0.9	22
228	Molecular dynamics simulation of thermal conductivity of single-wall carbon nanotubes. Physics Letters, Section A: General, Atomic and Solid State Physics, 2006, 350, 150-153.	2.1	65
229	Study on impurity desorption induced by femtosecond pulse laser based on a stochastic process model. Science in China Series D: Earth Sciences, 2006, 49, 78-88.	0.9	0
230	Thermal conductivity measurement of InGaAs/InGaAsP superlattice thin films. Science Bulletin, 2006, 51, 2931-2936.	1.7	11
231	Hydrodynamic lubrication in nanoscale bearings under high shear velocity. Journal of Chemical Physics, 2006, 125, 084702.	3.0	3
232	Monte Carlo Simulation of Silicon Nanowire Thermal Conductivity. Journal of Heat Transfer, 2005, 127, 1129-1137.	2.1	200
233	Minimum superlattice thermal conductivity from molecular dynamics. Physical Review B, 2005, 72, .	3.2	167

Monte Carlo Simulation of Thermal Conductivities of Silicon Nanowires. , 2005, , 397.

#	Article	IF	CITATIONS
235	Thermal expansion and impurity effects on lattice thermal conductivity of solid argon. Journal of Chemical Physics, 2004, 120, 3841-3846.	3.0	29
236	Molecular dynamics study of the lattice thermal conductivity of Kr/Ar superlattice nanowires. Physica B: Condensed Matter, 2004, 349, 270-280.	2.7	95
237	Molecular dynamics simulation of the meniscus formation between two surfaces. Applied Physics Letters, 2001, 79, 1267-1269.	3.3	11
238	Roughness Effects on Dynamic Response of High Density Disk Drives under High Knudsen Number. Tribology Transactions, 2001, 44, 179-184.	2.0	3
239	Cyclosporine-Containing Collagen Shields Suppress Corneal Allograft Rejection. American Journal of Ophthalmology, 1990, 109, 132-137.	3.3	46
240	Phonon dispersion relations of crystalline solids based on LAMMPS package. Chinese Physics B, O, , .	1.4	1